ARTICLE

Patterned Growth of Vertically Aligned Organic Nanowire Waveguide Arrays

Yong Sheng Zhao,[†,§] Peng Zhan,[‡,§] Jaemyung Kim,[†] Cheng Sun,[‡,*] and Jiaxing Huang[†,*]

[†]Department of Materials Science and Engineering and [‡]Department of Mechanical Engineering, Northwestern University, Evanston, Illinois 60208-3108. [§]These authors contributed equally to this work.

ABSTRACT Vertical nanowire arrays were prepared from an organic dye compound, 1,5-diaminoanthraquinone (DAAQ), on various types of substrates by a facile physical vapor transport method. It was found that the DAAQ grows much faster on the substrates with higher surface energies. Therefore, patterned growth of the nanowire arrays was achieved by modifying the substrate surfaces both geometrically and chemically to induce selective growth in areas of higher surface energies. The DAAQ nanowires can serve as nanosized active optical waveguides that allow the locally excited photoluminescence to propagate along the length of the wires. The low-loss waveguide propagation modes along the nanowire were observed experimentally. The nanowire arrays can be integrated directly with a portable fiber optics spectrometer for chemical vapor sensing.

KEYWORDS: organic nanowire · waveguide · vertical array · patterning · chemical sensor

Nanomaterials based on functional organic molecules have attracted increasing attention in the past few years.[1,2] Organic nanostructures offer some unique advantages such as relative ease of chemical doping,[3,4] high reactivity,[5] and good processability,[4] which make them complementary to their inorganic counterparts.[6] Applications of organic nanowires have been demonstrated in light-emitting diodes,[7] field-effect transistors,[8−10] chemical sensors,[11,12] optical waveguides,[13,14] and lasers.[15,16] While significant progress has been made in inorganic nanowire synthesis, where many methods to control the size, orientation, growth site and density of the nanowire arrays have been developed, much less has been done with organic nanowires. For example, ordered vertical arrays of inorganic nanowires have been fabricated and shown to be beneficial for many photonic and electronic devices.[17−20] However, vertical growth of organic nanowires has been rarely reported.[21,22] Site-selective growth of nanowires in predefined patterns has been proved to be able to simplify the device fabrication.[23,24] Owing to the relatively weak molecular interaction in organic nanostructures, their vapor transport can be done at relatively lower temperature. Therefore, site-selective, orientation-controlled synthesis of organic nanowire arrays should be very attractive since it could allow direct growth of these nanostructures onto prefabricated patterns for device integration.

Recently, we reported an example of the controlled growth of vertically aligned single crystal nanowire arrays from a small organic functional compound 1,5-diaminoanthraquinone (DAAQ, Scheme 1).[25] With a facile physical vapor transport method, we can prepare vertical nanowire arrays from DAAQ with controllable dimensions. Here we report patterned growth of these vertical nanowire arrays on substrates with predefined geometrical and chemical features. The nanowires can also be directly grown on sharp metal or AFM tips, and colloidal particles. Fluorescence microscopy and localized excitation experiments showed that the vertical DAAQ nanowires can act as miniaturized optical waveguides, which have much lower optical loss than the horizontal ones. In addition, the nanowire arrays were directly grown onto an optical fiber probe thus allowing real-time fluorescence measurement of these nanowires on exposure to chemical vapors.

RESULTS AND DISCUSSION

Self-seeded growth. The vapor transport growth of the DAAQ nanowires is considered to be controlled by vapor-solid (VS) process[6] as illustrated in Figure 1A. Figure 1B shows an SEM image of the early stage product of a DAAQ nanowire array grown

*Address correspondence to c-sun@northwestern.edu, jiaxing-huang@northwestern.edu.

Received for review November 5, 2009 and accepted January 28, 2010.

Published online February 8, 2010. 10.1021/nn901567z

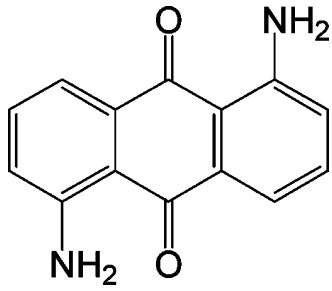

Scheme 1. Chemical Structure of 1,5-Diaminoanthraquinone Molecule

on a silicon wafer at 160 °C for 10 s. It can be seen that a layer of vertically aligned, elongated nanoparticles were already formed at the early stage of the vapor transport (Figure 1B, inset), which then act as the seeds for the epitaxial overgrowth of the wires. Figure 1C shows a SEM image showing the typical tilted view of the nanowire arrays grown at 160 °C for 5 min. The length and diameter of the DAAQ nanowires were controlled in large extension by altering the preparation conditions.[25] Longer wires can be prepared by increasing the growth time. For example, if the evaporation temperature is fixed at 160 °C, when 2, 5, 10, and 20 min of growth time are adopted, the lengths of the finally obtained nanowires are about 0.5, 1.5, 5, and more than 10 μm, respectively, without obvious variation in diameter. Moreover, DAAQ nanowires with larger diameters can be prepared by increasing the evaporation temperature. For example, at a fixed growth time of 5 min, evaporation temperatures of 160, 180, 200, and 220 °C result in nanowires of around 80, 100, 200, and more than 500 nm in diameter, respectively. Figure 1D is a transmission electron microscope (TEM) image showing the smooth surface and uniform width of a typical nanowire product. In our previous work,[25] the crystal structure of the DAAQ nanowires was determined to be a monoclinic lattice with $a = 3.78$ Å, $b = 9.73$ Å, $c = 15.01$ Å, $\beta = 82.4°$. The diffraction pattern of a single wire shown in the inset was indexed with this lattice, which indicates that the nanowires grew along the *a* axis of the DAAQ crystal.

DAAQ Nanowire Waveguides. The $\pi^* \rightarrow \pi$ type transition in the DAAQ molecules has a predominant intramolecular charge transfer character from amino groups to the carbonyl ones, which leads to strong fluorescence emission in visible region. Upon excitation, the resulting photoluminescence emission can be self-guided along the single crystalline DAAQ nanowires. Figure 1 panels E and F show the top and tilted view of the nanowire arrays under a fluorescence microscope upon excitation, respectively. Bright light was emitted from the tips of each wire under excitation. In the top view, only small emitting dots were observed, indicating good vertical alignment of the nanowires. In the tilted view, stronger fluorescence emission at the tips was revealed. The waveguided fluorescence can be best observed when the nanowires were transferred to lie horizontally on a substrate as shown in Figure 1G. The luminescence of DAAQ nanowires was much brighter at the tips and weaker from the wire bodies, which is a typical characteristic of optical waveguide. Nearly all of the observed wires exhibited this waveguiding behavior.

The waveguiding properties of the DAAQ nanowire were further studied with localized laser excitation at single nanowire level. A 488 nm laser was focused down to the diffraction limit to excite the nanowire locally. Then emission spectra at one end of the nanowire were measured as a function of the distance from the focused laser beam along the nanowire. Optical loss of

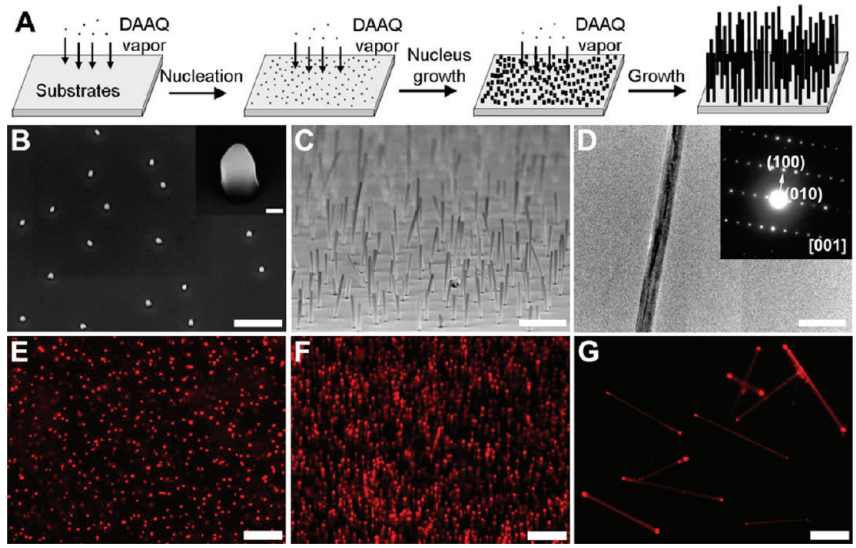

Figure 1. (A) Schematic illustration for the growth process of the vertical DAAQ nanowire arrays *via* vapor transport. Randomly arranged vertical nuclei serve as seeds to guide the further growth of the nanowires. (B) Tilted view (40°) SEM images of the DAAQ seeds grown at 160 °C for 10 s; scale bar is 2 μm. Inset: high magnification image; scale bar is 100 nm. (C) Tilted view (40°) SEM images of the DAAQ nanowire arrays grown at 160 °C for 5 min; scale bar is 1 μm. (D) TEM image of a single DAAQ nanowire showing a smooth surface of the nanowire; scale bar is 500 nm. Inset: SAED pattern reveals that the nanowire is single crystalline, grown in (100) direction. (E) Plane view and (F) tilt view PL microscopy image of the vertical DAAQ nanowire arrays, scale bars are 10 μm. (G) PL microscopy image of some isolated wires on glass, scale bar is 20 μm.

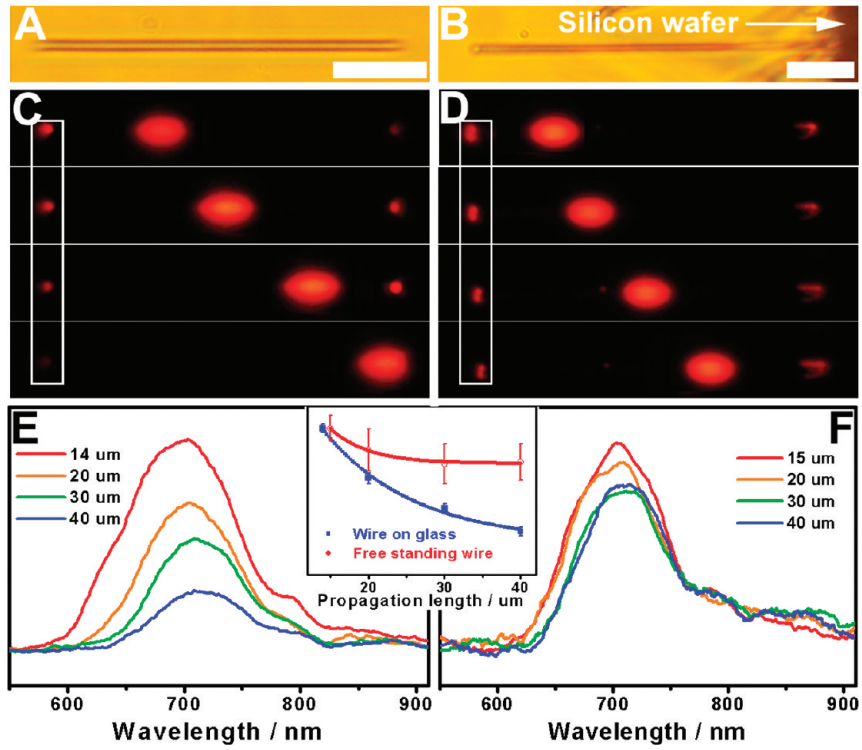

Figure 2. Bright field microscope image of (A) an isolated DAAQ nanowire on glass and (B) a single free-standing DAAQ wire vertically grown at the edge of a silicon wafer. Scale bars are 10 μm. (C and D) Microarea excited PL images of the two wires taken by exciting each wire at four different positions. (E and F) Spatially resolved PL spectra of the two samples obtained by exciting the wires at four different positions and collecting the outcoupling light at the wire tips as marked in panels C and D. Inset is the evanescent curves of the outcoupled emissions with the propagation lengths.

both horizontally placed nanowires and vertical ones was studied and compared. Figure 2 panels A and B are the bright field optical microscope images of an isolated DAAQ nanowire on glass, and a free-standing wire grown at the edge of silicon wafer (see Supporting Information, Figure S1), respectively. The diameters of both wires were around 500 nm. Figure 2 panels C and D are fluorescence images showing the two wires being excited locally with laser focused into a 5 μm spot at four different positions, respectively. The fluorescent guided fluorescence light is scattered at the end of the nanowire. A confocal microscopy setup was used to selectively collect the emission from the end of the nanowire with a 2 μm pinhole. The light is subsequently coupled to a grating spectrometer (Shamrock 303, Andor Technology) with matched TE-cooled EMCCD Camera. The laser spot is carefully positioned at the distance larger than 15 μm from the end of the nanowire to avoid direct photoluminescence emission at the point of excitation. Self-guided fluorescence propagated to the distal tips can be clearly observed in both types of nanowires as marked in the white boxes in Figure 2C,D. However, the emission intensity at the distal end of the horizontal nanowire decreased rapidly when the excitation spot was moved further away, indicating a significant optical loss for the propagating fluorescence. In contrast, the tip emission of the vertical wire exhibits much modest intensity variation, indicating much lower loss of the waveguide modes. The tip emission spectra corresponding to Figure 2 panels C and D are shown in Figure 2 panels E and F, respectively. The inset shows that the peak intensity of out-coupled emissions decays exponentially with the increase in propagation distance. The intensities were normalized against the emissions measured by the nearest excitation. The intensity distributed along the nanowire waveguide can be defined by $I(z) = I_0 e^{-2\beta z}$, where β is the attenuation constant.[26] It can be calculated from the decay curves that the attenuation constant of the horizontal wire on glass is 4.01×10^3 cm^{-1}, and that of the free-standing one is 1.74×10^3 cm^{-1}. The higher optical loss of the horizontal wires on glass is due to the energy leakage through the underlying substrates. However, such loss is minimized in the vertical nanowires. DAAQ films prepared by solution casting or vapor deposition are usually amorphous to polycrystalline, which are less favorable materials for waveguiding applications due to high scattering loss. Vertically aligned, single crystalline nanowires offer the best combination of materials and geometry in supporting the low loss waveguiding modes, which can potentially be used as optical interconnects.[27] The guided fluorescence emission of the wires was slightly red-shifted along the propagating length, which can be attributed to the reabsorption of the guided light during propagation.[13]

Site-Specific and Patterned Growth. During the vapor transport experiments, we noticed that the DAAQ tends to preferably nucleate and grow faster on high surface energy sites such as dust particles and scratches on sub-

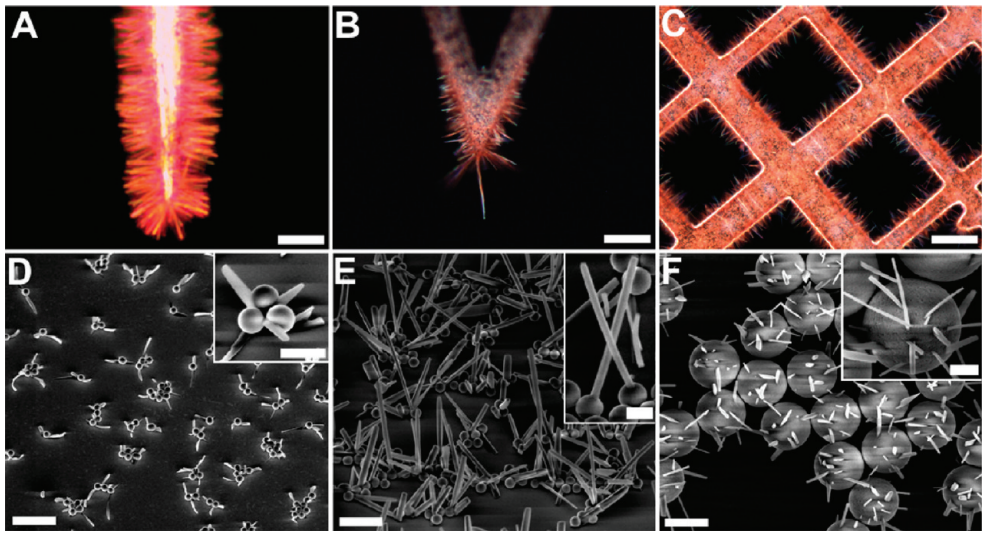

Figure 3. Optical microscopy images of DAAQ nanowires grown on (A) tungsten tip; (B) AFM tip; (C) the ridge of the TEM grids. Scale bars are 50 μm. SEM images of the DAAQ nanowires grown on the silicon wafers coated with silica spheres with diameters of (D) 350 nm, (E) 520 nm, and (F) 2.2 μm, respectively. Scale bars are 2 μm. Insets are the magnified images, scale bars are 500 nm.

strates. Vertical nanowire arrays can be grown on tungsten needles (Figure 3A) and on the ridges of a copper TEM grid (Figure 3C). Sharper tips or edges have higher surface energy due to smaller curvature, therefore tend to be the preferred sites for DAAQ deposition. For wires grown on AFM tips, oftentimes a much longer wire can be seen grown from near the very end of the tips as shown in Figure 3B. Another way to introduce high surface energy sites to a surface is by adding "dust" particles. Figure 3D−F are the SEM images showing DAAQ nanowires grown on silica beads deposited on a smooth silicon wafer. It can be seen that the DAAQ grew mainly on the spheres, which provided preferred nucleation centers for the DAAQ vapor. In comparison, no wires can be seen grown on the surface of silicon. The size of the silica particles affects the number of wires on each bead and their orientation. For the smallest spheres (350 nm, Figure 3D), the nanowires grew from the contact area between the sphere and the substrate, which should be the preferred condensation sites for DAAQ vapor. With larger spheres (520 nm, Figure 3E), the nanowires started to grow on the sphere surfaces. While only one or two wires were grown on the surface of the 520 nm spheres, multiple wires were obtained on bigger ones with diameter of 2.3 μm (Figure 3F). It is noteworthy that the length and diameter of the final nanowires are influenced by the temperature and the growth time, while not by the morphology or size of the nucleation centers.

The preferred nucleation and growth of DAAQ nanowires on high surface energy sites make it possible to grow ordered arrays on prepatterned substrates. For example, geometrical patterns on Si wafer can be made by scouring the surface to create alternating ridges and grooves as shown in Figure 4A,B. Here the ridge edges are higher surface energy sites due to much increased defects from scouring. Figure 4 panels C and D show the tilted and cross-sectional view SEM images of the DAAQ nanowire arrays grown on such patterned silicon wafers. DAAQ nanowires indeed grew selectively along the ridge edges. Although the surface

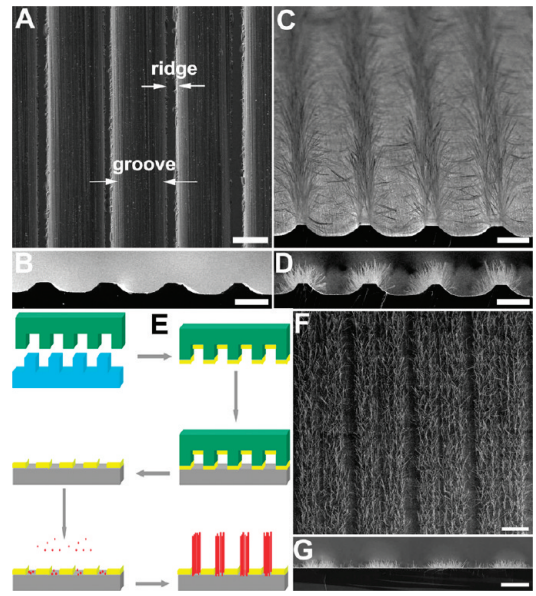

Figure 4. Selective growth of the DAAQ nanowires on the patterned substrates: (A) 40° tilt view and (B) cross sectional view SEM images of the silicon wafers prepatterned with periodic ridge-groove patterns by scouring using a dicing machine. Scale bars are 25 μm. (C) The 40° tilt view and (D) cross sectional view SEM images of the patterned growth of DAAQ nanowire arrays on silicon wafers prepatterned with periodic ridge-groove patterns by scouring using a dicing machine. Scale bars are 25 μm. (E) Schematic illustration for the PDMS patterned growth of the DAAQ nanowire arrays. Briefly, a PDMS stamp is molded to the relief pattern of a photoresist master. The stamp is then removed from the master and inked with FOTES. The stamp pattern is transferred to the silicon substrate, which is subsequently used for the growth of DAAQ. The nanowires tend to grow within the hydrophilic areas, resulting in a patterned vertical nanowire arrays. (F) The 40° tilt view and (G) cross sectional view SEM images of PDMS patterned growth of DAAQ nanowires. Scale bars are 50 μm.

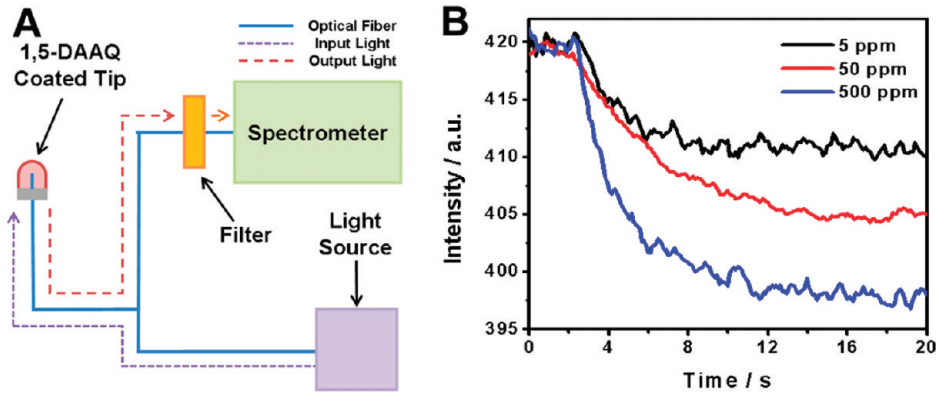

Figure 5. Demonstration of an acid vapor chemical sensor utilizing the fluorescence quenching of the DAAQ nanowire arrays. (A) Schematic illustration of the setup for the sensing measurement. The nanowires coated on a tip were excited with 365 nm light and the resulting fluorescence signal was detected with a spectrometer. (B) The PL intensities of the nanowires monitored at 685 nm when exposed to HCl vapors of 5, 50, and 500 ppm, respectively. A minute amount of HCl vapor can be detected within few seconds of exposure.

of the grooves were also very rough, very little wires were found there likely due to depletion of DAAQ vapor molecules. The fluorescence microscopy images (Supporting Information, Figure S2) also show very bright, waveguided tip emissions.

Microcontact printing can pattern the surface with self-assembled monolayers corresponding to different surface energy, which can also direct the growth of nanowires. The SiO_2-coated silicon substrates were first treated with 1:1:5 volume ratio of ammonium, hydrogen peroxide, and deionized water to be hydrophilic. Then a polydimethylsiloxane (PDMS) stamp with patterns of lines and separations was inked with (tridecafluoro-1,1,2,2-tetrahydrooctyl)triethoxysilane (FOTES), and pressed onto the wafers for 5 min (Figure 4E). This creates alternative hydrophilic/hydrophobic domains on the substrates. Since the unstamped, hydrophilic areas have higher free energy, the preferred condensation would deplete the DAAQ vapor molecules available to the hydrophobic domains. The resulting patterned nanowire arrays are shown in the SEM images of Figure 4F,G. The preferred growth of DAAQ on hydrophilic surface was confirmed in a control experiment, where the amounts of deposited DAAQ on a hydrophilic and a hydrophobic glass slides were compared by UV−vis spectra (Supporting Information, Figure S3).

As was reported in our previous work,[25] DAAQ nanowires have much improved sensing performance over bulk materials on exposure to acidic and basic chemical vapors. As shown in Figure 3, DAAQ nanowires can grow on a great variety of solid surfaces. This makes it possible to directly integrate DAAQ nanowires onto a sensing device such as a portable fiber optics spectrometer (Figure 5A) for real-time chemical detection. The fluorescence of the coated nanowires can be monitored on exposure to acidic and basic vapors. Figure 5B shows the changes in the fluorescence intensities of DAAQ nanowires measured when exposed to HCl vapors of 5, 50, and 500 ppm, respectively. The nanowires were able to detect HCl vapor at all these concentrations while DAAQ powders composed of micrometer-sized particles would not be sensitive enough to show measurable changes. The fluorescence of the quenched nanowires can be recovered in air to around 95% of their original intensity in about 2 h. Moreover, they can also be rapidly reset by basic vapors (*e.g.*, NH_3) within a few seconds, which also provides a mechanism for detecting basic vapors. The basic vapor can deprotonate the amine groups and help to restore the intramolecular charge transfer, leading to the recovery of color and fluorescence.[28]

CONCLUSION

Vertical organic nanowire arrays of DAAQ dye molecules were prepared by a facile physical vapor transport method. The DAAQ nanowires can serve as nanosized optical waveguides, and the optical loss of the vertical wires is much lower compared to that of the horizontally placed wires on glass substrates. DAAQ grows much faster on the substrates with higher surface energies. Based on this, patterned growth of the nanowire arrays was achieved by both microcontact printing and a physical scouring method. The as-prepared nanowire arrays were also integrated to sensing devices for the detection of trace amounts of acidic vapors with very high sensitivity.

METHODS

The model compound used in this work, DAAQ, was purchased from TCI (D 076). The hydrochloric acid (GR) and ammonia (GR) were purchased from EMD Chemicals, Inc. The silica microspheres were purchased from Bangs Laboratories, Inc. The FOTES was purchased from Gelest. All chemicals were used without further treatment.

The DAAQ nanowire arrays were prepared with a physical vapor transport method. In a typical preparation, 10 mg DAAQ powder was dissolved with ethanol in a 100 mL 2-necked flask. The flask was then put into a silicon oil bath and the temperature was increased to 60 °C to evaporate the ethanol. The flask was rotated to ensure that a uniform layer of DAAQ film was obtained. Then a solid substrate (silicon wafer with native oxide

layer, glass, glass fiber, Au foil, Fe foil, Al foil, Cu wire, or W needle) was perpendicularly mounted to suspend on top of the solid sample (see Supporting Information, Figure S4 for the setup). The oil bath was subsequently heated to the desired evaporation temperature as monitored by a thermometer inserted into the flask from one neck. After deposition, the substrate was removed from the flask and a layer of vertically aligned nanowire arrays were observed under microscopes. The vaporization can be carried out in flowing air, nitrogen, or under vacuum. The morphology and chemical composition of the final nanowire products appeared to be insensitive to the atmosphere used.

The patterned growth of the DAAQ nanowire arrays was achieved by both physically and chemically patterning the silicon substrates with alternate areas of higher and lower surface energies before the vapor transport. The physical patterning was carried out by scouring the silicon wafers with alternate ridges and grooves. Then the scoured wafers were washed with DI water and isopropyl alcohol to remove the silicon dusts. The washed wafers were subsequently treated with 1:1:5 volume ratio of ammonium, hydrogen peroxide, and DI water before used for the growth of DAAQ nanowires.

The chemical patterning was performed through microcontact printing[29] with PDMS stamps with patterns of lines and separations. First, a piece of stamp was washed with acetone, ethanol, and DI water sequentially. Then the stamp was treated hydrophilic with 1:1:5 volume ratio of ammonium, hydrogen peroxide, and DI water. After 1 h, the stamp was taken out and dried with nitrogen, and subsequently exposed to the saturated vapor of FOTES for 30 min. Then the stamp was pressed onto a piece of hydrophilically treated silicon wafer for 5 min to generate alternating hydrophobic and hydrophilic stripes for the patterned growth of nanowire arrays.

The as-prepared nanowire arrays were characterized by scanning electron microscope (SEM, FEI Nova Nano 600), transmission electron microscope (TEM, Hitachi HF-8100), UV−vis spectrometer (Beckman, DU 520), fluorescence spectrophotometer (Hitachi F-4500), and fluorescence microscope (Nikon TE2000 U). To measure the PL spectra of single nanowires, the nanowires were excited with a focused laser with 488 nm wavelength (Argon Laser, Spectra Physics). The PL spectra were collected with an objective dispersed onto grating spectrograph with matched TE-cooled CCD camera (Shamrock 303, Andor Technology).

The fluorescence of the DAAQ nanowire arrays was monitored *in situ* and in real time by integrating them with an optical fiber coupled into a spectrometer. In the chemical sensing experiments, the nanowire arrays were exposed to the vapor of HCl aqueous solutions of various concentrations. The concentration of HCl vapor was calculated based on ref 30. For example, the HCl vapor concentration above 2.4 M HCl solution is about 5 ppm.[30] Then the fluorescence of the nanowires were recovered by exposing them in air about 2 h or in the vapor of a 5% ammonia solution for a few seconds.

Acknowledgment. The work was supported by a seed grant from the National Science Foundation Nanoscale Science and Engineering Center at Northwestern (NSF EEC-0647560), the American Chemical Society Petroleum Research Fund (48678-G10), and National Science Foundation Nanoscale Science and Engineering Center for Scalable and Integrated Nanomanufacturing (NSF CMMI-0751621). J.K. also thanks the Initiative for Sustainability and Energy at Northwestern (ISEN) for a graduate fellowship. TEM and electron diffraction were performed in the EPIC facility of the Northwestern Atomic & Nanoscale Characterization Experimental (NUANCE) Center. We thank Dr. Jinsong Wu for help with the TEM measurements.

Supporting Information Available: Optical microscope images of the vertical DAAQ nanowires used for waveguide measurements; SEM images of the silicon wafers pretreated with scouring; PL microscope image of the physically patterned nanowire arrays; UV−vis absorption spectra taken from the DAAQ nanowire arrays grown on the hydrophilic and hydrophobic parts of the same cover glass; schematic illustration of the synthetic setup. This material is available free of charge *via* the Internet at http://pubs.acs.org.

REFERENCES AND NOTES

1. Zhao, Y. S.; Fu, H. B.; Peng, A. D.; Ma, Y.; Xiao, D. B.; Yao, J. N. Low-Dimensional Nanomaterials Based on Small Organic Molecules: Preparation and Optoelectronic Properties. *Adv. Mater.* **2008**, *20*, 2859–2876.
2. Zang, L.; Che, Y. K.; Moore, J. S. One-Dimensional Self-Assembly of Planar Pi-Conjugated Molecules: Adaptable Building Blocks for Organic Nanodevices. *Acc. Chem. Res.* **2008**, *41*, 1596–1608.
3. Zhao, Y. S.; Fu, H. B.; Hu, F. Q.; Peng, A. D.; Yang, W. S.; Yao, J. N. Tunable Emission from Binary Organic One-Dimensional Nanomaterials: An Alternative Approach to White-Light Emission. *Adv. Mater.* **2008**, *20*, 79–83.
4. Peng, A. D.; Xiao, D. B.; Ma, Y.; Yang, W. S.; Yao, J. N. Tunable Emission from Doped 1,3,5-Triphenyl-2-Pyrazoline Organic Nanoparticles. *Adv. Mater.* **2005**, *17*, 2070–2073.
5. Lim, S. J.; An, B. K.; Jung, S. D.; Chung, M. A.; Park, S. Y. Photoswitchable Organic Nanoparticles and a Polymer Film Employing Multifunctional Molecules with Enhanced Fluorescence Emission and Bistable Photochromism. *Angew. Chem., Int. Ed.* **2004**, *43*, 6346–6350.
6. Xia, Y. N.; Yang, P. D.; Sun, Y. G.; Wu, Y. Y.; Mayers, B.; Gates, B.; Yin, Y. D.; Kim, F.; Yan, Y. Q. One-Dimensional Nanostructures: Synthesis, Characterization, and Applications. *Adv. Mater.* **2003**, *15*, 353–389.
7. Zhao, Y. S.; Di, C. A.; Yang, W. S.; Yu, G.; Liu, Y. Q.; Yao, J. N. Photoluminescence and Electroluminescence from Tris(8-Hydroxyquinoline)Aluminum Nanowires Prepared by Adsorbent-Assisted Physical Vapor Deposition. *Adv. Funct. Mater.* **2006**, *16*, 1985–1991.
8. Briseno, A. L.; Mannsfeld, S. C. B.; Lu, X. M.; Xiong, Y. J.; Jenekhe, S. A.; Bao, Z. N.; Xia, Y. N. Fabrication of Field-Effect Transistors from Hexathiapentacene Single-Crystal Nanowires. *Nano Lett.* **2007**, *7*, 668–675.
9. Xiao, S. X.; Tang, J. Y.; Beetz, T.; Guo, X. F.; Tremblay, N.; Siegrist, T.; Zhu, Y. M.; Steigerwald, M.; Nuckolls, C. Transferring Self-Assembled, Nanoscale Cables into Electrical Devices. *J. Am. Chem. Soc.* **2006**, *128*, 10700–10701.
10. Tang, Q. X.; Li, H. X.; He, M.; Hu, W. P.; Liu, C. M.; Chen, K. Q.; Wang, C.; Liu, Y. Q.; Zhu, D. B. Low Threshold Voltage Transistors Based on Individual Single-Crystalline Submicrometer-Sized Ribbons of Copper Phthalocyanine. *Adv. Mater.* **2006**, *18*, 65–68.
11. Naddo, T.; Che, Y. K.; Zhang, W.; Balakrishnan, K.; Yang, X. M.; Yen, M.; Zhao, J. C.; Moore, J. S.; Zang, L. Detection of Explosives with a Fluorescent Nanofibril Film. *J. Am. Chem. Soc.* **2007**, *129*, 6978–6979.
12. Che, Y. K.; Yang, X. M.; Loser, S.; Zang, L. Expedient Vapor Probing of Organic Amines Using Fluorescent Nanofibers Fabricated from an N-Type Organic Semiconductor. *Nano Lett.* **2008**, *8*, 2219–2223.
13. Zhao, Y. S.; Xu, J. J.; Peng, A. D.; Fu, H. B.; Ma, Y.; Jiang, L.; Yao, J. N. Optical Waveguide Based on Crystalline Organic Microtubes and Microrods. *Angew. Chem., Int. Ed.* **2008**, *47*, 7301–7305.
14. Takazawa, K.; Kitahama, Y.; Kimura, Y.; Kido, G. Optical Waveguide Self-Assembled from Organic Dye Molecules in Solution. *Nano Lett.* **2005**, *5*, 1293–1296.
15. O'Carroll, D.; Lieberwirth, I.; Redmond, G. Microcavity Effects and Optically Pumped Lasing in Single Conjugated Polymer Nanowires. *Nat. Nanotechnol.* **2007**, *2*, 180–184.
16. Zhao, Y. S.; Peng, A. D.; Fu, H. B.; Ma, Y.; Yao, J. N. Nanowire Waveguides and Ultraviolet Lasers Based on Small Organic Molecules. *Adv. Mater.* **2008**, *20*, 1661–1665.
17. Hochbaum, A. I.; Fan, R.; He, R. R.; Yang, P. D. Controlled Growth of Si Nanowire Arrays for Device Integration. *Nano Lett.* **2005**, *5*, 457–460.
18. Wang, Z. L.; Song, J. H. Piezoelectric Nanogenerators Based on Zinc Oxide Nanowire Arrays. *Science* **2006**, *312*, 242–246.
19. Park, W. I.; Yi, G. C. Electroluminescence in N-ZnO Nanorod Arrays Vertically Grown on P-GaN. *Adv. Mater.* **2004**, *16*, 87–90.

20. McAlpine, M. C.; Ahmad, H.; Wang, D. W.; Heath, J. R. Highly Ordered Nanowire Arrays on Plastic Substrates for Ultrasensitive Flexible Chemical Sensors. *Nat. Mater.* **2007**, *6*, 379–384.
21. Chung, J. W.; An, B. K.; Kim, J. W.; Kim, J. J.; Park, S. Y. Self-Assembled Perpendicular Growth of Organic Nanoneedles *via* Simple Vapor-Phase Deposition: One-Step Fabrication of a Superhydrophobic Surface. *Chem. Commun.* **2008**, 2998–3000.
22. Ryu, J.; Park, C. B. High-Temperature Self-Assembly of Peptides into Vertically Well-Aligned Nanowires by Aniline Vapor. *Adv. Mater.* **2008**, *20*, 3754–3758.
23. Huang, M. H.; Mao, S.; Feick, H.; Yan, H. Q.; Wu, Y. Y.; Kind, H.; Weber, E.; Russo, R.; Yang, P. D. Room-Temperature Ultraviolet Nanowire Nanolasers. *Science* **2001**, *292*, 1897–1899.
24. Ng, H. T.; Han, J.; Yamada, T.; Nguyen, P.; Chen, Y. P.; Meyyappan, M. Single Crystal Nanowire Vertical Surround-Gate Field-Effect Transistor. *Nano Lett.* **2004**, *4*, 1247–1252.
25. Zhao, Y. S.; Wu, J. S.; Huang, J. X. Vertical Organic Nanowire Arrays: Controlled Synthesis and Chemical Sensors. *J. Am. Chem. Soc.* **2009**, *131*, 3158–3159.
26. Jackson, J. D. , *Classical Electrodynamics,* 3rd ed.; Wiley: New York, 1999; p xxi, 808.
27. Yan, R. X.; Gargas, D.; Yang, P. D. Nanowire Photonics. *Nat. Photon.* **2009**, *3*, 569–576.
28. Huss, A. S.; Pappenfus, T.; Bohnsack, J.; Burand, M.; Mann, K. R.; Blank, D. A. The Influence of Internal Charge Transfer on Nonradiative Decay in Substituted Terthiophenes. *J. Phys. Chem. A* **2009**, *113*, 10202–10210.
29. Xia, Y. N.; Whitesides, G. M. Soft Lithography. *Angew. Chem., Int. Ed.* **1998**, *37*, 551–575.
30. Fritz, J. J.; Fuget, C. R. Vapor Pressure of Aqueous Hydrogen Chloride Solutions, 0 to 50 °C. *Ind. Eng. Chem. Chem. Eng. Data Ser.* **2002**, *1*, 10–12.